Residual shear strength of saturated sand and silt – an energy approach

La force résiduelles de cisailles de sable saturé et s'envase – une approche d'énergie

R. Singh, D. Roy and K. Chiranjeevi

Indian Institute of Technology, Kharagpur, India

ABSTRACT

The residual shear strengths of saturated sandy and silty soils are often estimated from the relationships between insitu penetration resistances and residual shear strength obtained from the back analysis of post failure geometries of embankments that suffered varying degrees of distress resulting from static rapid (undrained) loading. The procedures for back analysis employed so far do not account for viscous drag and strain energy. A simple procedure has been proposed herein approximately accounting for viscosity and strain energy. The results from back analysis of ten flow failure case histories using the proposed energy approach were used to develop a correlation between residual shear strength and Standard Penetration Test (SPT) blow counts.

RÉSUMÉ

Les forces résiduelles de cisailles de sable saturé et de sols de silty sont souvent estimées des relations entre les résistances de pénétration d'insitu et de la force de cisailles résiduelle a obtenu de l'analyse arrière de géométries d'échec de poste de remblais qui a souffert variant des degrés de résulter de détresse du rapide statique (undrained) chargeant. Les procédures pour de retour l'analyse salariée loin ne représente pas si visqueux traîne et tend de l'énergie. Une procédure simple a été proposée qu'en ceci représente approximativement l'énergie de viscosité et tension. Les résultats de de retour l'analyse de dix histoires de cas d'échec de flux utilisant l'approche d'énergie proposée a été utilisée pour développer une corrélation entre la force de cisailles résiduelle et le Test de Pénétration Standard (SPT) les comptes de coup.

Keywords: Residual shear strength, sand and silty soils, energy approach.

1 INTRODUCTION

The residual shear strengths, s_u of dams and embankments underlain by the saturated sand and silty soils are often estimated from the correlations between s_u estimated from back analysis of earth structures that suffered significant distress due to undrained loading episodes and cone tip resistance, standard penetration test (SPT) blow count or shear wave velocity (Seed 1987; Davies et al. 1988; Seed and Harder 1990; Stark and Mesri 1992; Fear and Robertson 1995; Wride et al. 1999; Olson and Stark 2002; and Olson and Stark 2003). The back analysis procedures used so far do not account for the viscous nature of liquefied soil and the strain energy associated with large deformations normally arise in a flow failure. A simple energy-based procedure for back analysis has been proposed herein for estimating the residual shear strengths of non plastic soils, which takes an approximate account of the viscous behavior of soils participating in flow failure and the strain energy associated with large deformations.

The proposed approach is based on the concept of equating the potential energy prior to the triggering of flow slide to the dissipation of energy during the failure of the earth structures. The total dissipation energy during failure was estimated considering the distortional strain energy and the energy loss due to friction and viscous drag approximately. The details of the procedure are described in the following sections.

2 REVIEW OF AVAILABLE PROCEDURES

Because of the strong influence of sampling disturbance on the undrained deformation behavior of non plastic soils and the difficulty in extracting undisturbed sample for laboratory testing, the undrained residual shear strength are usually estimated from back analyses of earth structures that suffered damages during episodes of rapid loading. The estimates of back analyses are usually related to the cone tip resistance measured during a piezocone penetration test, SPT blow count or shear wave velocity. Based on the premise that the residual shear strength of non plastic soils at large strains depends uniquely on the pre-deformation void ratio, Seed (1987) developed a procedure for assessing the stability of embankments constructed on or comprising liquefiable materials. The procedure was based on a relationship between clean-sand equivalent stress-normalized and energy-corrected SPT blow count, $(N_1)_{60}$, and residual shear strength developed from limit equilibrium back analyses of unstable slopes and embankments. The correlations were updated by Seed et al. (1988) and Seed and Harder (1990).

Davis et al. (1988) used a different conceptual model for back analysis based on the consideration that the unbalanced force arising as a result of drop of shear strength is balanced by the decrease in driving force due to deformation of earth structure. The procedure assumes that the locus of the center of gravity of the mobilized mass is hyperbolic, that the soil behavior is isotropic, and that the unbalanced force arises instantaneously as the shear strength drops with the rise of pore water pressure and the soil mass is mobilized.

The shear strength ratio, s_u/σ'_v, works better as a measure of soil strength than the shear strength only (Stark and Mesri 1992; Ishihara 1993; Wride et al. 1999; Olson and Stark 2002; Idriss and Boulanger 2007). Therefore, Stark and Mesri (1992) relates the clean-sand equivalent, normalized SPT blow count, $(N_1)_{60}$, and s_u/σ'_v from static limit equilibrium back analyses of post failure geometries of earth embankments.

Since the residual shear strength, s_u as well as the normalized shear wave velocity, V_{s1}, depends on void ratio Fear and Robertson (1995) proposed a set of semi-empirical correlations between s_u and V_{s1}. These correlations, based primarily on laboratory data from testing of reconstituted soil samples, were found to depend on compressibility and somewhat weakly on the coefficient of lateral earth pressure at rest, K_0. Since the correlation between shear wave velocity and void ratio is tenuous and the residual shear strength represents

Proceedings of the 17th International Conference on Soil Mechanics and Geotechnical Engineering
M. Hamza et al. (Eds.)

doi:10.3233/978-1-60750-031-5-3447

large strain soil behavior whereas shear wave velocity is a small strain measurement, an inference drawn from this approach is likely to be imprecise (Roy et al. 1996).

Olson and Stark (2002, 2003) developed correlations between normalized cone tip resistance, q_{c1}, and normalized Standard Penetration tests (SPT) blow counts, $(N_1)_{60}$ and yield and residual shear strength ratio, s_u/σ'_v by back analyzing twenty-nine embankment failure case histories.

3 PROPOSED PROCEDURE FOR BACK ANALYSIS

As discussed earlier, the back analyses procedures used so far do not account for the viscous nature of non plastic soils after triggering of flow failure. Nor do they account for the strain energy associated with large deformations normally arise during a flow failure. The procedure described in the following sub sections takes an approximate account of viscosity and strain energy. The approach is based on energy balancing: The flow slide is considered to be driven when the sliding mass settles from a state of higher potential energy to a state of lower potential energy. The difference in potential energy between the initial and final configurations are dissipated in work done against cohesive frictional and viscous components of resistance at the base of the sliding mass and in accumulation of strain energy.

3.1 *Mapping*

The post failure soil mass is first mapped back to their pre failure positions. For mapping, the post failure geometry of an earth structure is divided into several slices (Figure 1). The area segment adjacent to the toe of the post failure configuration (Slice 1: Figure 1) is mapped back to the toe of the pre failure geometry considering volumetric scaling, i.e.,

$$V_{1p} = \left(V_p / V_f\right) \times V_{1f} \tag{1}$$

where V_{1p} and V_{1f} are the volumes of slice 1 in the pre and post failure configurations, respectively, and V_p *and* V_f are the volumes of the entire slide mass in the pre and post failure configurations, respectively. The slices further away from the toe of slide are then mapped sequentially in a similar manner.

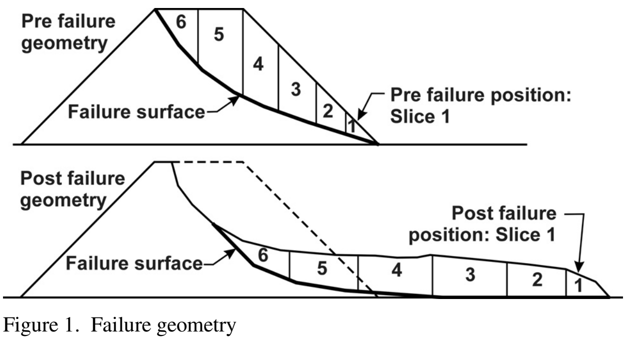

Figure 1. Failure geometry

3.2 *Potential energy*

For estimating the loss of potential energy that drives the flow slide, the weight of each individual slice was first multiplied by the elevation difference between the centers of gravity of pre and post failure configurations of the slice. The products were then summed for all the slices to obtain the total loss of potential energy.

3.3 *Strain energy*

The shear strain for each slice was estimated by first transforming the pre and post failure slice configurations into equivalent rectangles and measuring the rotation of the leading diagonal of these transformed slice configurations. The operation is illustrated in Figure 2 using Slice 4 of Figure 1.

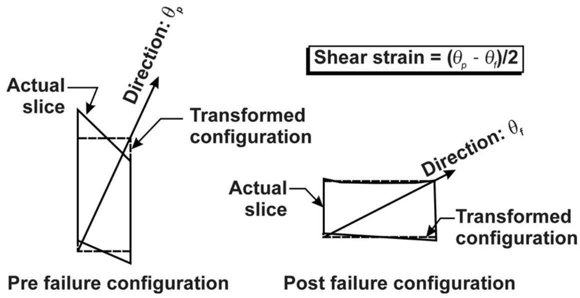

Figure 2. Shear strain estimation

The shear stresses corresponding to average slice-base inclination were estimated for each slice following Perloff et al. (1967). These stresses were multiplied with the shear strain estimates of the slices for obtaining the strain energy for each slice. The total strain energy developed during the deformation process was estimated by summing the strain energies of all slices. The volumetric strain energy is not considered in this procedure.

3.4 *Energy loss at the base of the silde mass*

The energy that drives the flow slide is expended partly in the work done against the shear strength at the base of the sliding mass. The corresponding energy loss was estimated assuming mobilization of residual undrained shear strength at the base of the slice if the soil is expected to behave in a contractive manner and liquefy. For dilative and non-liquefiable soils, e.g., dense sand and silt, and sand and silt above water table, the frictional energy loss was estimated considering drained friction angle. The shear strength was assumed to be isotropic.

3.5 *Viscous drag*

The mobilized shear strength at the slice base that resists the flow failure has two components: static resistance and viscous drag. Slide masses typically move at a velocity of 20 km/hour (111 m/s) to 30 km/hour (167 m/s) e.g. Aberfan Tip No. 4 and 7 (Lucia, 1981). This corresponds to a viscous drag equal to about the static shear strength as illustrated in Figure 3 (de Alba

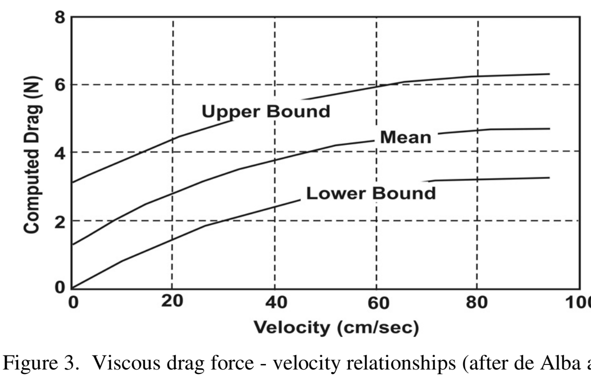

Figure 3. Viscous drag force - velocity relationships (after de Alba and Ballestero 2006)

and Ballestero 2006). Assuming the drag force at zero velocity to represent the static shearing resistance mobilized at slide base, the static shearing resistance was arithmetically scaled up by the factor 1.25 to account for viscous drag.

3.6 *Estimation of residual s_u*

To estimate the residual shear strength, s_u from the back analysis, the shear strength ratio, s_u/σ'_v was varied in such a way that the total potential energy loss during the flow slide becomes equal to the total dissipated energy during the deformation process.

4 ADVANTAGES OF THE PROPOSED PROCEDURE

The proposed procedure takes an approximate account of cohesive frictional as well as viscous material behavior, the strain energy accumulation that accompanies large deformations typical of flow slides and three dimensional failure geometries. Towards this the actual slice widths were considered for estimating the resistance due to shear strength mobilization at the base of the unstable soil mass. Although in this study, material behavior was assumed as isotropic, the proposed procedure can accommodate anisotropic shear strength behavior by using residual shear strengths in accordance with the slice base inclination following a scheme similar to that reported in Singh et al. (2008).

5 BACK ANALYSIS

Ten incidents of flow slides found in the literature have been back analyzed using the procedure proposed in the preceding sections (Table 1). The computed residual undrained shear strengths obtained in the exercise are summarized in Table 2. Also included in Table 2 for comparison are the residual undrained shear strengths obtained by others from back analyses of these case histories.

Table 1. Back analyzed flow slides

Case histories	$(N_1)_{60}$	Reference
1. Calaveras dam	11.0	Hazen 1918
2. Eckersley	8.0	Hungr 1995
3. Fort Peck dam	9.0	Konard and Watts 1995
4. Jamuna Bridge	11.3	Yoshomine et al. 1999
5. Lake Ackerman	8.0	Hryciw et al. 1990
6. Merriespurit Tailings dam	9.0	Fourie and Papageorgiou 2001
7. Nerlerk Slide 4	9.1	Sladen et al. 1985
8. North dike	11.3	Olson and Stark 2000
9. Sullivan Mine	7.0	Davies et al. 1998
10. Uetsu Line	3.0	Yamada 1966

The back analyzed case histories involve flow failure of saturated non plastic soils. The shear strength of these soils and penetration resistances depends upon the relative density of the soil deposit and compressibility of the soil grains during undrained loading (Vaid and Chern 1985; Robertson and Campanella 1986). The main factors affecting grain compressibility are grain size, grain angularity, and crushability. In general, soils containing larger amounts of finer, angular or crushable particles exhibit greater compressibility and smaller undrained shear strength. Thus, a correlation between s_u/σ'_v and stress normalized penetration resistance, $(N_1)_{60}$, is expected to depend on soil grain compressibility unless the penetration resistance is corrected to eliminate the influence of grain compressibility.

Table 2. Comparison of residual shear strengths

Case histories	This study	Stark and Mesri (1992)	Olson and Stark (2003)
Calaveras Dam	0.080	0.101	0.112
Eckersley	0.160	-	-
Fort Peck Dam	0.063	0.054	0.077
Jamuna Bridge	0.082	-	-
Lake Ackerman	0.161	0.219	0.075
Merriespurit tailings dam	0.028	-	-
Nerlerk Slide 4	0.048	-	-
North Dike	0.124	-	0.106
Sullivan Mine	0.100	-	-
Uetsu Line	0.019	0.028	0.028

In this study the stress normalized penetration resistances were by and large found to be smaller for soils with greater grain compressibility compared to the soils with smaller grain compressibility. Consequently, the penetration resistances were not only normalized here for overburden pressure as indicated earlier but also for soil grain compressibility according to the simple procedure outlined below:

Examination of a database of calibration chamber tests of cone penetration assembled by Robertson and Campanella (1986) indicates that for sands with relative densities smaller than 40 %, the cone tip resistances for low and medium compressibility sands are about 2.00 and 1.50 times that for highly compressible sand, respectively. The corresponding factors for 60 % relative density were estimated to be 1.28 and 1.20, respectively. For the intermediate relative densities, the linear interpolation scheme is used.

The penetration resistances measured in deposits known to be composed of grains of high and medium compressibility were corrected to obtain the "low compressibility equivalent" by multiplying the measured penetration resistances by the factors listed above in accordance with the estimated relative density of the deposit except as indicated below:

Soils with fines contents greater than 50 % were considered highly compressible irrespective of their relative density, grain angularity or depositional environment and soils composed primarily of angular or crushable grains were also considered highly compressible.

For applying the correction, where direct estimates of relative density were unavailable, the relative densities were estimated following Jamiolkowski et al. (1988).

A correlation between residual undrained shear strength ratio, s_u/σ'_v, and compressibility corrected Standard Penetration Test (SPT) blow counts, $(N_1)_{60c}$ is presented in Figure 4. The mean relationship shown in the figure was obtained by non linear regression. The upper and lower bound relationships were obtained by manual scaling of the mean relationship. The correlation obtained in this study is compared with those obtained by Olson and Stark (2002) and Stark and Mesri (1992) in Figure 5.

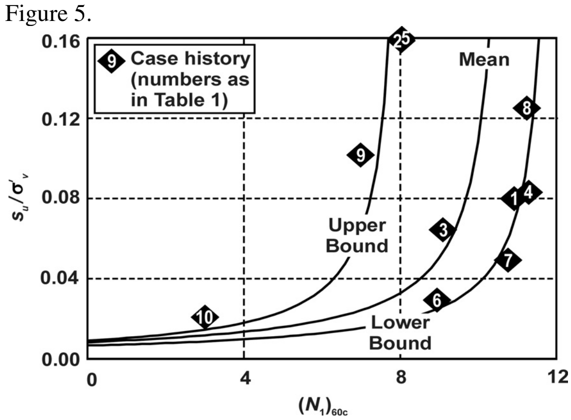

Figure 4. s_u/σ'_v - $(N_1)_{60c}$ relationship

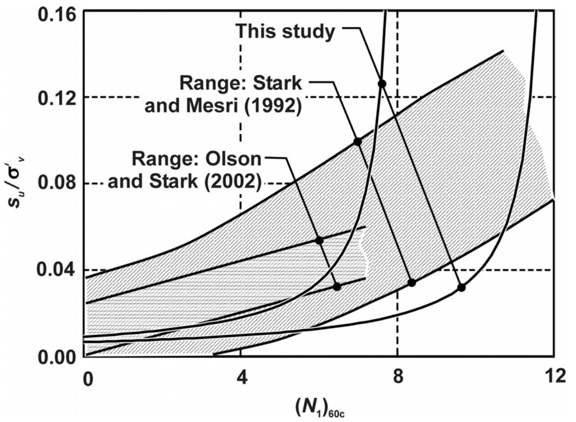

Figure 5. Comparison of s_u/σ'_v - $(N_1)_{60c}$ relationships

6 CONCLUSIONS

A procedure based on energy balance has been proposed in this study for back analysis of distressed earth structures for estimating the residual shear strengths of non plastic soils. The proposed approach equates the potential energy released during the failure to approximate estimation of energy dissipated because of cohesive frictional and viscous components of material strength and strain energy associated with distortion. Although the approach is simple, it is capable of accommodating three dimensional failure geometries and material anisotropy. The procedure has been used to back analyze ten incidents of failure of earth structures initiated because of rapid loading to estimate the residual undrained shear strengths. Based on the results, correlations have been developed between the undrained shear strength ratio and compressibility corrected and stress normalized SPT blow count. The results have also been compared with those obtained by others based on conventional limit equilibrium back analyses.

REFERENCES

Davis, A.P., Poulos, S.J., and Castro, G. 1988. Strengths backfigured from liquefaction case histories, Proceedings, 2nd International Conference on Case Histories in Geotechnical Engineering, pp. 1693-1701.

Davies, M. P., Dawson, B. B., and Chin, B. G. 1998. Static liquefaction slump of mine tailings – A case history, Proceedings, 51st Canadian Geotechnical Conference.

de Alba, P., and Ballestero, T. P. 2006. Residual shear strength after liquefaction: A rheological approach, Journal of Soil Dynamics and Earthquake Engineering, Vol. 26, pp. 143-151.

Fear, C.E., and Robertson, P.K. 1995. Estimation of undrained strength of sand: a theoretical framework, Canadian Geotechnical Journal, Vol. 32, pp. 859-870.

Fourie, A.B., and Papageorgiou, G. 2001. Define an appropriate steady state line for Merriespruit gold tailings, Canadian Geotechnical Journal, Vol. 38, pp. 695-706

Hazen, A. 1918. A study of the slip in the Calaveras Dam, Engineering News Records, No. 81, pp. 1158-1164.

Hryciew, R. D., Vitton, S., and Thomann, T. G. 1990. Liquefaction and flow failure during seismic exploration, Journal of Geotechnical Engineering, Vol. 116, pp. 1881-1899.

Hungr, O. 1995. A model for the runout analysis of rapid flowslides, debris flows, and avalanches, Canadian Geotechnical Journal, Vol. 32, pp. 610-623.

Idriss, I.M., and Boulanger, R.W. 2007. SPT- and CPT- based relationships for the residual shear strength of liquefied soils, Proceedings, 4th Int. Conf. on Earthquake Geotech. Engrg., Thessaloniki, Greece, Springer, The Netherlands, K.D. Pitilakis, ed. June 25-28, 2007, pp. 1-21.

Ishihara, K. 1993. Liquefaction and flow failure during earthquakes, Géotechique, Vol. 43, No. 3, pp. 351-415.

Jamiolkowski, M., Ghionna, V.N., Lancellotta, R., and Pasqualini, E. 1988. New correlations of penetration tests for design practice. De Ruiter, J., Ed., Penetration Testing 1988, A.A. Balkema, Rotterdam, the Netherlands, 1988, Vol. 1, pp. 263-296.

Konard, J. M., and Watts, B. D. 1995. Undrained shear strength for liquefaction flow failure analysis, Canadian Geotechnical Journal, Vol. 33, pp. 784-794.

Lucia, P.C. 1981. Review of experiences with the flow failures of tailings dams and waste impoundments. PhD Dissertation, University of California, Berkeley, USA.

Olson, S. M., and Stark, T. D. 2000. Static liquefaction flow failure of the North Dike of Wachusett Dam, Journal of Geotechnical and Geoenvironmental Engineering, Vol. 126, pp. 1184-1193.

Olson, S. M., and Stark, T. D. 2002. Liquefied strength ratio from liquefied flow failure case histories, Canadian Geotechnical Journal, Vol. 39, pp. 629-647.

Olson, S. M., and Stark, T. D. 2003. Yield strength ratio and liquefaction analysis of slopes and embankments, Journal of Geotechnical and Geoenvironmental Engineering, ASCE, Vol. 129, No. 8, pp. 727-737.

Perloff, W.H., Baladi, G.Y., and Herr, M.E. 1967. Stress distribution within and under long elastic embankments, Highway Research Record No. 181.

Robertson, P.K., and Campanella, R.G. 1986. Guidelines for use, interpretation and application of the CPT and CPTU. Soil Mechanics Series No. 105, Department of Civil Engineering, University of British Columbia, Vancouver.

Roy, D., Campanella, R.G., Byrne, P.M., and Hughes, J. 1996. Strain level and uncertainty of liquefaction related index tests. Uncertainty in the Geologic Environment: from Theory to Practice, Shackelford, C.D., Nelson, P.P., and Roth, M.J.S., eds., Geotechnical Special Publication No. 58, ASCE, 2, 1149-1162.

Seed, H.B. 1987. Design problems in soil liquefaction. Journal of Geotechnical Engineering, ASCE, Vol. 113, pp. 827-845.

Seed, H.B., Seed, R.B., Harder, L.F., and Jong, H.-L. 1988. Re-evaluation of the slide in the Lower San Fernando Dam in the earthquake of February 9, 1971, Rep. No. UCB/EERC-88/04, University of California, Berkeley, April.

Seed, R.B., and Harder, L.F., Jr. 1990. SPT-based analysis of cyclic pore pressure generation and undrained residual strength. Proceedings, H.B. Seed Memorial Symposium, Bi-Tech Publishing Ltd., Vol. 2, pp. 351–376.

Singh, R., Mitra, D., Kumar, M., and Roy, D. 2008. Correlations between undrained shear strength and penetration resistance for anisotropic sand and silt. Proceedings, 3rd Int. Conf. on Site Characterization, Taipei, Taiwan, Taylor & Francis, 1173-1179.

Sladen, J. A., D'Hollader, R. D., and Krahn, J. 1985. The liquefaction of sands, a critical collapse surface approach, Canadian Geotechnical Journal, Vol. 22, pp. 564-578.

Stark, T.D., and Mesri, G. 1992. Undrained shear strength of liquefied sand for stability analysis, Journal of Geotechnical Engineering, Vol. 118, 1727-1747.

Vaid, Y.P., and Chern, J.C. 1985. Cyclic and monotonic undrained response of saturated sands. ASCE National Convention, Detroit, pp. 120-147.

Yamada, G. 1966. Damage to earth structures and foundations by the Niigata earthquake June 16, 1964, Soils and Foundations, Vol. 6, No. 1, pp. 1-13.

Yoshimine, M., Robertson, P. K., and (Fear) Wride, C. E. 1999. Undrained shear strength of clean sands to trigger flow liquefaction, Canadian Geotechnical Journal, Vol. 36, No. 3, pp. 891-906.

Yoshimine, M., Ishihara, K., and Vargas, W. 1998. Effects of principal stress direction and intermediate stress on undrained shear behavior of sand. Soils and Foundation, Vol. 38, pp. 179-188.

Wride, C.E., McRoberts, E.C. and Robertson, P.K. 1999. Reconsideration of case histories for estimating undrained strength in sandy soils, Canadian Geotechnal Journal, Vol. 39, pp. 907-933.